

The Optical Model Applied to Calculate High Energy Neutron Scattering Cross-Section Using “SCAT2”

Wint Shwe War Hlaing

Abstract

Theoretical studies of systematic of neutron scattering cross sections on various materials for neutron energy up to several MeV are of practical importance. In this work, total cross-section of neutrons of very high energy (2-20 MeV) using Statistical Optical Model code SCAT2 were calculated. The calculated cross-sections with those given in Evaluated Nuclear Data File (ENDF-VI) were also compared.

Key words: Neutron Cross-Sections, Optical Model, Nuclear Code, SCAT2

Introduction

Nuclear cross-section data are needed for scientific works as well as for reactor construction. Nuclear cross-section data are provided by experimental works. Nuclear experiments are very expensive, so model calculations are used to predict cross-sections. Various nuclear codes are developed to calculate nuclear cross-sections. Not all the codes are perfect and we have to find correction factors. Generally, nuclear cross-sections depend on target mass, incident energy and type of incident particle.

In this work we have tried to compare the SCAT2 cross-section and ENDF-VI cross-sections to investigate the validity of the code. The calculation of cross-section is made on S-matrix, which are defined as

$$\bar{\sigma}_c^{EL} = |\bar{1} - \bar{S}_{cc}|^2 = |1 - \bar{S}_{cc}|^2 = \sigma_c^{SE}$$

is the average inelastic cross-section,

$$\sigma_c^{inel} = \sigma_c^t - \sigma_c^{EL} \approx \left(1 - |S_{cc}|^2\right) = \sigma_c^{ABS}$$

The real and imaginary parts of S_{cc} can be obtained from the fact that there the energy dependence of S_{cc} is given by,

$$S_{cc} = e^{-2i\phi_c} \left[1 - i \sum_{\mu} \frac{\Gamma_{\mu c}}{E - E_{\mu} + i\Gamma/2} \right]$$

Where all the symbol are real parameter, we have

$$\bar{S}_{cc} = e^{-2i\phi_c} \left[1 - \frac{\pi \langle \Gamma_{\mu c} \rangle_{\mu}}{D} \right]$$

Materials and Methods

Calculation procedure

As the SCAT2 runs under DOS, we have to load the DOS. After loading DOS, we have to load the SCAT2 program. Under SCAT2 program we open INPUT.DAT and make some changes to input data file (Oliver, 1984).

```
C:\>SCAT2> EDIT SCAT2TST.DAT ↵
```

The file is saved and closed. The calculation is done when we type this command.

```
C:\>SCAT2>SCAT2 ↵
```

To see and edit output results, we open SCAT2 and rename it.

```
C:\>SCAT2>EDIT SCAT2TST.LST ↵
```

The statistical model for nuclear reactions

In the study of nuclear reactions the concept of the compound nucleus (the statistical model for nuclear reactions) is not always reliable. The statistical nature of the compound nucleus theory implies that its predictions are at best averages, and do not take into account the differences between specific nuclei. Therefore a more detailed model is needed for the description of nuclear reactions (Aung Kyi Myint, 2004; <http://www.t2lanl.gov>, 2005).

The statistical model assumes that the compound nucleus is formed immediately when the incident neutron reaches the nuclear surface. The cross-section for reaching the surface turns out to be a monotonically decreasing function of the energy, varying as $E^{-1/2}$ for small energies and reaching the asymptotic value $2\pi R^2$ for large energies. At the neutron energies involved, between 0.1MeV and several MeV and for intermediate or heavy nuclei, individual resonances cannot be resolved and the measured cross-sections are averages over many levels.

The optical model for nuclear reactions

The optical model describes the effect of the nucleus on the incident particle by a potential well $-V_0(r)$, but allows for the possibility of compound nucleus formation by adding to the potential a negative imaginary part, $-iV_1(r)$. This part produces absorption of the incident particle within the nucleus, and this absorption is supposed to represent the formation of the compound nucleus.

The basic task of nuclear-reaction theory is to find a solution of the Schrödinger equation of the system under consideration that satisfies the appropriate boundary conditions. This Schrödinger equation is a particle one, so that the total wave function depends on the coordinates of all the interacting particles, and the potential is the sum of all the interactions between them. To solve such an equation is an almost impossible task, so at the outset we assume that the interaction between the incident particle and the target nucleus can be represented by a simple one-body potential $V(r)$, where r is their separation. This assumption may be partly justified by considering the single-particle shell model, and the general form of $V(r)$ can be found. Throughout the analysis we work in the centre of mass system, with the exception that by convention the energy of the incident particle is quoted in the laboratory system (Ganesan, 1991).

On the optical model, compound nucleus formation does not occur immediately or with complete certainty. Even if the incident particle has entered the nucleus, it is removed from its free particle state only with some delay and with a certain probability. The model has

also been extended and applied with more complicated potential functions to other nuclear reactions and cross-sections.

The feature of nuclear scattering cross-sections can be explained by a very simple model in which we represent the interaction between the incident nucleons and the nucleus by a one body potential that depends only on the nuclear radius. This is called the optical model.

Optical model analysis of elastic scattering

The optical model potential can be used to calculate the differential cross-section for the elastic scattering of nucleons by nuclei making use of the quantum mechanical scattering formalism. This calculation gives only the direct elastic scattering so the comparison with the experimental cross-section must only be made at energies high enough for the compound elastic cross-section to be negligible (Aye Myat Mynn, 2004).

The potential experienced by a particle incident on a nucleus is the extension to positive energies of the shell-model potential for bound nucleons. The full optical potential is

$$V(r) = V_c(r) + U f_u(r) + i w f_w(r) + V_{so}(r)$$

$$V_c(r) = \frac{Z_I Z_T e^2}{2R_c} \left(3 - \frac{r^2}{R_c^2}\right), \quad r < R_c$$

$$V_c(r) = \frac{Z_I Z_T e^2}{r}, \quad r > R_c$$

where Z_I and Z_T are the charges of the incident particle and target nucleus.

The Coulomb potential $V_c(r)$ is that of a charged particle in the electrostatic field of the nucleus. This is calculable from the nuclear charge distribution, but in practice it is sufficiently accurate to use the potential due to a sphere of radius R_c with its charge uniformly spread throughout its volume (Enge, 1975).

The real part of the potential is due to the action of all the nucleons in the nucleus on the incident particle, and is thus approximately given by

$$U(r) = \sum_i V(|r - r_i|) \approx \int \rho(r') V(|r - r'|) dr'$$

where $\rho(r')$ is the nuclear density and $V(|r - r'|)$ the effective interaction between the incident particle and a nucleon in the nucleus. Since the nucleon-nucleon interaction has short range, it can be expressed by a delta function, giving,

$$V(r) \approx \int \rho(r') V_0 \delta(r - r') dr' = U_0 \rho(r)$$

Thus to first approximation we expect the optical potential to have a radial variation that follows the nuclear density quite closely, with perhaps a somewhat greater radius reflecting the finite range of the nucleon-nucleon interaction. It is useful to represent this radial dependence by an appropriate analytical expression, and for this purpose the Saxon-Woods form is particularly convenient so the real potential becomes

$$U(r) = U f_u(r) = \frac{u}{1 + \exp\left(\frac{r - R}{a}\right)}$$

where R is the radius and a is the surface diffuseness parameter.

The nucleon-nucleon interaction is purely real, so this argument applies only to the real part of the nucleon optical potential. The real and imaginary parts of the optical potential have the same form, and this is still widely followed. Since the imaginary potential takes into account in a global way all the non-elastic processes that remove flux from the elastic channel it is not possible to establish its form by simple physical arguments. The best fits are obtained by adding to the volume imaginary potential a surface-peaked potential of the radial derivative form.

$$g(r) = -4a \frac{df(r)}{dr} = \frac{4 \exp\left(\frac{r-R}{a}\right)}{\left[1 + \exp\left(\frac{r-R}{a}\right)\right]^2}$$

where the factor 4a is introduced to ensure that $g(R) = 1$.

The imaginary part of the potential increases in magnitude with the energy is to take account of the increasing cross-sections of the various non-elastic reactions.

These radial forms for the nucleon optical potential sufficed until quite recently, when evidence from proton elastic scattering indicated the need for a modified form at higher energies.

The optical model can be applied to the scattering of deuterons, tritons, alpha-particles and heavier nuclei. Many optical model analyses have been made of the elastic scattering of deuterons, hellions, tritons and alpha-particles by nuclei. As for nucleons, the depths of the real and imaginary parts of the potential, and of the spin-dependent terms are found to vary smoothly with energy and from one nucleus to another (Kaplan, 1962).

Results

The calculated data and respective graphs are shown in the following slides (Shamu & Ferguson, 2000);

Table 1. Total Cross-section of ${}^9_4\text{Be}$

E (MeV)	Scat2 Cs(b)	Jendls CS(b)	Error (%)
2.0000	1.5190	2.0568	-26.14
4.0000	1.5052	1.7953	-16.16
6.0000	1.5018	1.5356	-2.20
8.0000	1.4948	1.5340	-2.55
10.0000	1.5034	1.4956	0.53
12.0000	1.5139	1.4951	1.26
14.0000	1.5106	1.4667	3.00
16.0000	1.4908	1.4451	3.16
18.0000	1.4596	1.4457	0.96
20.0000	1.4225	1.4177	0.34

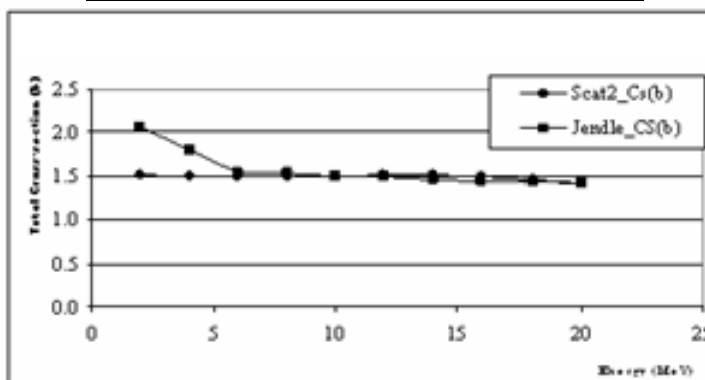


Figure 1 Comparison of Total CS of SCAT2 and JENDL 3.2 for ${}^9_4\text{Be}$

Table 2. Total Cross-section of $^{24}_{12}\text{Mg}$

E (MeV)	Scat2_Cs(b)	Jendle_CS(b)	Error (%)
2.0000	3.4124	2.3020	48.24
4.0000	2.4204	1.8436	31.28
6.0000	1.9678	1.5257	28.98
8.0000	1.7661	1.6569	6.59
10.0000	1.7184	1.6021	7.26
12.0000	1.7250	1.7410	-0.92
14.0000	1.7397	1.7651	-1.44
16.0000	1.7696	1.8118	-2.33
18.0000	1.8178	1.8275	-0.53
20.0000	1.8743	1.8090	3.61

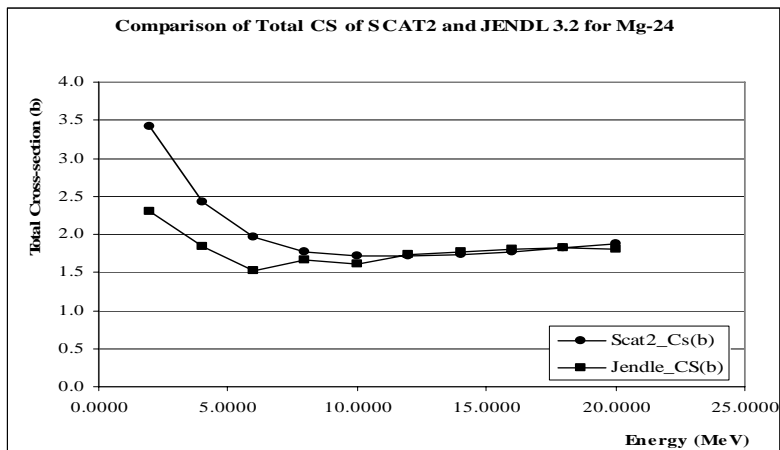


Figure 2 Comparison of Total CS of SCAT2 and JENDL 3.2 for $^{24}_{12}\text{Mg}$

Table 3 Total Cross-section of $^{52}_{24}\text{Cr}$

E (MeV)	Scat2_Cs(b)	Jendle_CS(b)	Error (%)
2.0000	3.7866	3.6863	2.72
4.0000	3.7638	3.8325	-1.79
6.0000	3.6403	3.6416	-0.03
8.0000	3.3566	3.3424	0.43
10.0000	3.0121	2.9608	1.73
12.0000	2.6804	2.6325	1.82
14.0000	2.4369	2.4191	0.74
16.0000	2.3006	2.3007	0.00
18.0000	2.2321	2.2518	-0.88
20.0000	2.1944	2.2313	-1.65

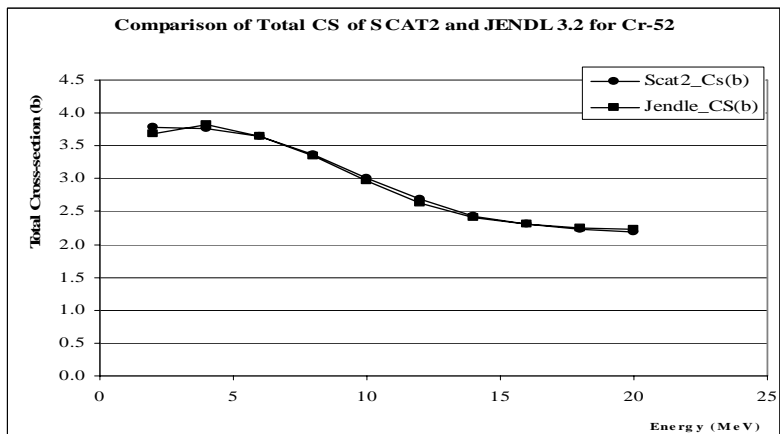


Figure 3 Comparison of Total CS of SCAT2 and JENDL 3.2 for $^{52}_{24}\text{Cr}$

Table 4. Total Cross-section of $^{58}_{28}Ni$

E (MeV)	Scat2_Cs(b)	Jendle_CS(b)	Error (%)
2.0000	3.5693	3.0783	15.95
4.0000	3.7497	3.5977	4.22
6.0000	3.8509	3.8059	1.18
8.0000	3.6251	3.5896	0.99
10.0000	3.2745	3.2781	-0.11
12.0000	2.9455	3.0064	-2.02
14.0000	2.7051	2.7613	-2.03
16.0000	2.5319	2.5692	-1.45
18.0000	2.3909	2.4253	-1.42
20.0000	2.2947	2.3751	-3.39

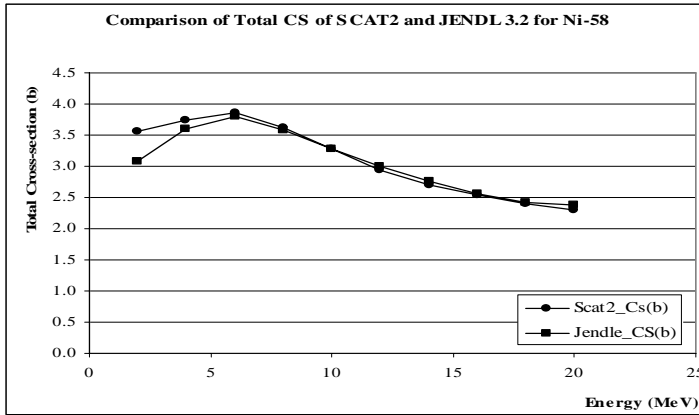


Figure 4 Comparison of Total CS of SCAT2 and JENDL 3.2 for $^{58}_{28}Ni$

Table 5. Total Cross-section of $^{232}_{90}Th$

E (MeV)	Scat2_Cs(b)	Jendle_CS(b)	Error (%)
2.0000	6.8042	7.0400	-3.35
4.0000	7.2661	7.8800	-7.79
6.0000	7.0620	6.9800	1.18
8.0000	6.2278	6.0800	2.43
10.0000	5.5002	5.6200	-2.13
12.0000	5.2774	5.6300	-6.26
14.0000	5.3568	5.7400	-6.68
16.0000	5.5783	5.9900	-6.87
18.0000	5.8793	6.2700	-6.23
20.0000	6.1407	6.4100	-4.20

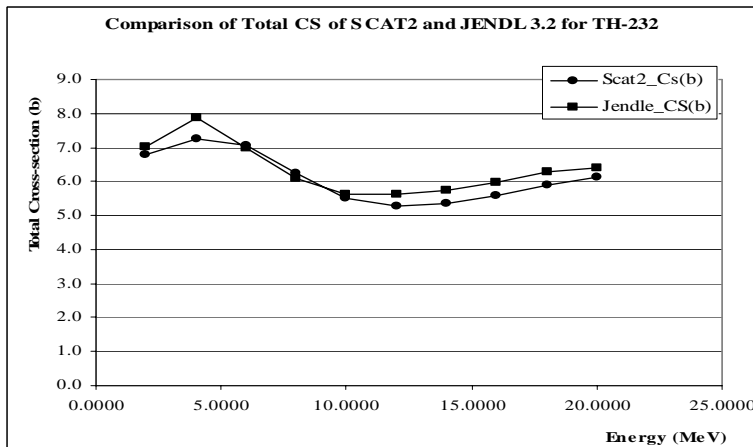


Figure 5 Comparison of Total CS of SCAT2 and JENDL 3.2 for $^{232}_{90}Th$

Table 6. Total Cross-section of $^{238}_{92}\text{U}$

E (MeV)	Scat2_Cs(b)	Jendle_CS(b)	Error (%)
2.0000	6.8072	7.3440	-7.31
4.0000	7.2079	7.9750	-9.62
6.0000	7.2668	7.1290	1.93
8.0000	6.4628	6.4260	0.57
10.0000	5.7296	5.9610	-3.88
12.0000	5.4264	5.8020	-6.47
14.0000	5.3974	5.8990	-8.50
16.0000	5.5910	6.0780	-8.01
18.0000	5.9142	6.1790	-4.29
20.0000	6.1941	6.2750	-1.29

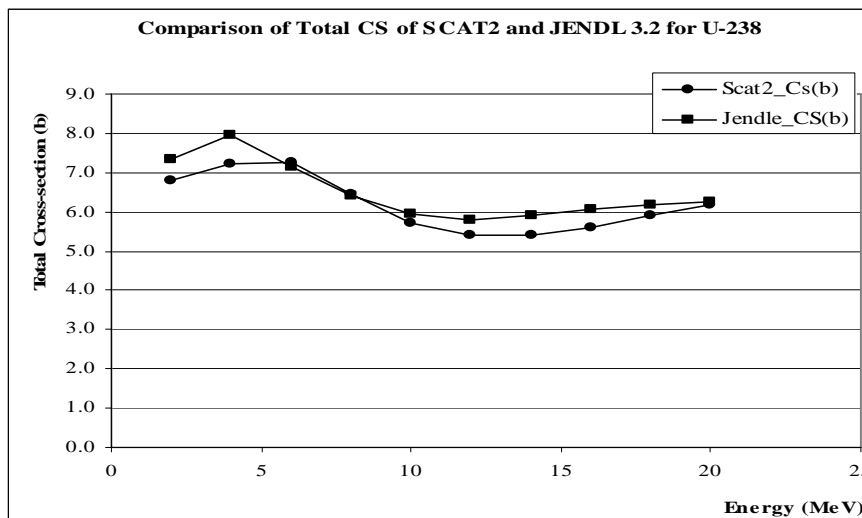


Figure 6 Comparison of Total CS of SCAT2 and JENDL 3.2 for $^{238}_{92}\text{U}$

Discussion

The comparison of total cross-sections obtained by SCAT2 and that of JENDL for ^9_4Be is given in Table 1 and Figure 1. From the graph we can see that the results obtained by SCAT2 data are a bit different from ENDF data in low energy and exactly the same in high energy range.

The comparison of total cross-sections obtained by SCAT2 and that of JENDL for $^{24}_{12}\text{Mg}$ is given in Table 2 and Figure 2. From the graph we can see that the results obtained by SCAT2 data are a bit different from ENDF data in low energy and exactly the same in high energy range.

The comparison of total cross-sections obtained by SCAT2 and that of JENDL for $^{52}_{24}\text{Cr}$ is given in Table 3 and Figure 3. From the graph we can see that the results obtained by two codes are exactly the same.

The comparison of total cross-sections obtained by SCAT2 and that of JENDL for $^{58}_{28}\text{Ni}$ is given in Table 4 and Figure 4. From the graph we can see that the results obtained by two codes are quite the same, but exactly the same in high energy range.

The comparison of total cross-sections obtained by SCAT2 and that of JENDL for ${}^{232}_{90}\text{Th}$ is given in Table 5 and Figure 5. From the graph we can see that the results obtained by two codes are quite the same.

The comparison of total cross-sections obtained by SCAT2 and that of JENDL for ${}^{238}_{92}\text{U}$ 92-U-238 is given in Table 6 and Figure 6. From the graph we can see that the results obtained by two codes are quite the same.

Conclusion

It is found that the cross-sections obtained by calculations of IAEA nuclear code SCAT2 well agree with those obtained given in JENDL 3.2 of ENDF-VI especially for very high energy neutron. The results are valid for various targets. The code is also applicable for light nuclides, intermediate nuclides and heavy nuclides. Thus, SCAT2 is an efficient tool for the determination of nuclear cross-sections and other useful nuclear information.

Acknowledgements

I would like to express my profound thanks to Dr. Tin Tun Myint, and Dr. Si Si Hla Bu, Pro-Rectors, Hinthada University, for their kind permission and encouragement to carry out this work.

It is my pleasure to express my sincere thanks to Professor Dr. Mya Mya Win, Head of Department of Physics, Hinthada University, for her kind permission to carry out this work and her keen interest and help given during this research work.

Special thanks are also due to my supervisor Dr. Win Sin, Assistant Lecturer, Department of Physics, Taungoo University, for his criticism of the manuscript.

References

- Aung Kyi Myint (2004). *Optical model parameter generator*, PhD Thesis, Yangon University.
- Aye Myat Mynn (2004). *Calculation and analysis of neutron cross-sections using IAEA nuclear code SCAT2 with different energy ranges*, PhD Thesis, Yangon University.
- Enge, H. A. (1975). *Introduction to nuclear physics*, (London: Addison-Wesley).
- Ganesan, S. (1991). *ABAREX, Optical-Statistical Model* (OECD NEA Data Bank: PSR 248/ABAREX)
- Kaplan, I. (1962). *Nuclear physics* (New York: Addison-Wesley).
- Oliver, B. (1984). *SCAT2:UN PROGRAMME DE MODELE OPTIQUE SPHERIQUE* (Centre d'Etudes de Bruyeres-le-Chatel)
- Shamu, R. E, and Ferguson, S. M. (2000). *Computation of Neutron Cross Sections from 15 MeV to 200 MeV for $A \geq 40$* , viewed on 15th March 2006, <http://www.fjfi.cvut.cz/con_adtt99/papers/mo-O-C15.pdf>

The Web site <http://www.t2lanl.gov>, *Nuclear Information Service*, 12.1.2005